This is a repository copy of *Picosecond time-resolved infrared spectroscopy of rhodium and iridium azides*.

White Rose Research Online URL for this paper:
http://eprints.whiterose.ac.uk/109109/

Version: Accepted Version

Article:
Portius, P. orcid.org/0000-0001-8133-8860, Meijer, A. J. H. M., Towrie, M. et al. (2 more authors) (2014) Picosecond time-resolved infrared spectroscopy of rhodium and iridium azides. Dalton Transactions, 43 (47). pp. 17694-17702. ISSN 1477-9226

https://doi.org/10.1039/c4dt02097a

Reuse
Unless indicated otherwise, fulltext items are protected by copyright with all rights reserved. The copyright exception in section 29 of the Copyright, Designs and Patents Act 1988 allows the making of a single copy solely for the purpose of non-commercial research or private study within the limits of fair dealing. The publisher or other rights-holder may allow further reproduction and re-use of this version - refer to the White Rose Research Online record for this item. Where records identify the publisher as the copyright holder, users can verify any specific terms of use on the publisher's website.

Takedown
If you consider content in White Rose Research Online to be in breach of UK law, please notify us by emailing eprints@whiterose.ac.uk including the URL of the record and the reason for the withdrawal request.

eprints@whiterose.ac.uk
https://eprints.whiterose.ac.uk/

Picosecond time-resolved infrared spectroscopy of rhodium and iridium azides

Peter Portius*,[1] Anthony J. H. M. Meijer,[1] Michael Towrie,[2] Benjamin F. Crozier,[1] Ingrid Schiager[1]

Picosecond time-resolved infrared spectroscopy was used to elucidate early photochemical processes in the diazido complexes $M(Cp^*)(N_3)_2(PPh_3)$, M = Rh (**1**), Ir (**2**), using 266 nm and 400 nm excitation in THF, CH_2Cl_2, MeCN and toluene solutions. The time-resolved data have been interpreted with the aid of DFT calculations on vibrational spectra of the singlet ground states and triplet excited states and their rotamers. While the yields of phototransformations *via* N_2 loss are low in both complexes, **2** cleaves a N_3 ligand under 266 nm excitation. The molecular structure of **1** is also reported as determined by single crystal X-ray diffraction.

Introduction

Azides play a prominent role in photochemical transformations[1,2] and photo-induced catalysis[3] involving organic and inorganic azides as well as azido complexes. Detailed photochemical studies of transition metal azido complexes revealed photo-induced reductive eliminations[4-8] with mechanisms reminiscent of photo-induced C-H bond activation reactions observed with transition metal carbonyl complexes.[9-14] These reactions were studied in inert matrices,[15,16] in solution[17-21] and in the gas phase.[22] A primary step in the photolysis of azido complexes may involve the initial elimination of N_2 from an excited state and the formation of highly reactive nitrenes, which is usually followed by the addition of electron-rich species in solution or rearrangement *via* insertion reactions.[23] The formation of nitrido complexes and the reductive elimination of the azidyl radical are alternative photochemical responses.[7,24] Reactions involving azides can be monitored conveniently since the symmetric and asymmetric stretching vibrations of the linear N_3 group, $\nu_{as}(N_3)$ and $\nu_s(N_3)$ give rise to intense absorption bands in the mid-IR spectral region. The spectral position of these bands is sensitive to structural and electronic changes which makes time-resolved infrared (TRIR) spectroscopy a suitable technique to study the nature and the photochemistry of the photogenerated excited states.[26,27] Using transient absorbance (TA) and time-resolved infrared (TRIR) spectroscopies, a variety of azides has been investigated,[25] including, for example, mono- and bis(phosphine) diazido platinum(II) complexes. In these experiments, a coordinatively unsaturated species, $Pt(N_3)(PPh_3)_2$, was identified as highly reactive intermediate. Investigations of the iridium complex $Ir(Cp^*)(N_3)_2(PPh_3)$, $Cp^* = C_5Me_5$, involved the continuous irradiation of benzene solutions at λ_{exc} = 313 nm,[9] which produced $Ir(Cp^*)H(Ph)(PPh_3)$ and $Ir(Cp^*)H\{(\mu\text{-}Ph)PPh_2\}(PPh_3)$ in reductive elimination / C-H insertion and orthometallation reactions. In halogenated solvents, however, the photo-reaction generates the chloro complex $Ir(Cp^*)Cl_2(PPh_3)$ *via* N_3 / Cl ligand exchange. In a related investigation near-ultraviolet radiation generates $Ir(Cp^*)(L)$ as a reactive intermediate, which undergoes oxidative addition with solvent C-H and C-Cl bonds.[5] The quantum yields for these reactions range from 0.01 to 0.3. The lack of mechanistic insight on the ultrafast time scale motivated our investigation of late transition metal azido complexes as part of a wider research programme into nitrogen-rich energetic compounds.[28-30] This work describes the first pico-second TRIR (ps-TRIR) spectroscopic study on these complexes using $Rh(Cp^*)(N_3)_2(PPh_3)$ and $Ir(Cp^*)(N_3)_2(PPh_3)$.

Results and Discussion

Spectroscopy

The complexes subject to this investigation, $M(Cp^*)(N_3)_2(PPh_3)$, M = Rh (**1**), Ir (**2**), are shown in Scheme 1. The UV/vis absorption spectra in MeCN (Fig. 1) feature two resolved bands at 393 nm and 269 nm (with the extinction coefficients 6.1×10^3 and 2.0×10^4 l mol^{-1} cm^{-1}, respectively) for complex **1**, whilst the spectrum of complex **2** exhibits one band at 305 nm (3.7×10^3 l mol^{-1} cm^{-1}). The band positions of **1** are slightly solvent dependent with shifts of less than 300 to 500 cm^{-1} (λ_{max} [nm] = 397, 272, DMF; 398, 272, THF; 398, 273, CH_2Cl_2).

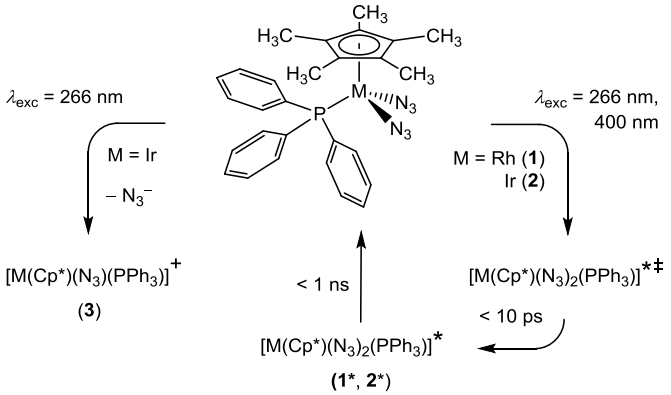

Scheme 1. Photoreactions triggered by excitation at 400 nm and 266 nm, ~120 fs pulse , M = Rh, Ir; * electronic excited state; *‡ vibrationally excited electronic excited state.

The FTIR spectra of **1** and **2** (presented in the bottom panels of Fig.s 2 and 4) in the mid-IR region are dominated by two (**1**) or three (**2**) extensively overlapping absorption bands arising from asymmetric in-phase and out-of-phase azide N-N-N stretching vibrations, $\nu_{as}(N_3)$, which in MeCN solution are centred at 2026 and 2007 cm^{-1} (**1**) and 2037 and 2017 cm^{-1} (**2**), respectively. The ps-TRIR spectra were obtained in the spectral range between *ca.* 1850 and 2150 cm^{-1} in MeCN, CH_2Cl_2, THF and toluene under 400 nm and 266 nm, ~120 femtosecond excitation (see Table 1).

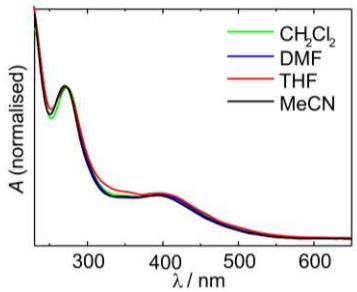

Figure 1. UV/*vis* absorption spectra of complex **1**.

The TRIR spectra (Fig. 2) of $Rh(Cp^*)(N_3)_2(PPh_3)$ (**1**) in MeCN under 400 nm excitation show the fully bleached ground state $\nu_{as}(N_3)$ bands (denoted as feature "a" in Fig. 2) at 2 ps after excitation, and a broad and initially featureless transient absorption centred at 1977 cm^{-1}. This transient band decays rapidly while giving rise to new, only partially overlapping transient bands (b) which are fully formed 15 ps after excitation while no transient absorption remains at low wavenumbers ("c", <1950 cm^{-1}). These transients decay within the following 800 ps – a process which is accompanied by the simultaneous recovery of the parent bands. Precise band positions, approximate shapes and time-dependent areas were obtained by deconvoluting the spectra using *pseudo* Voigt profiles. This treatment afforded kinetic data in spectral regions affected by band overlap (see Fig.s 9 and S3-6) according to which three individual transient bands centred at 2003 cm^{-1}, 1983 cm^{-1} and 1969 cm^{-1} rise with a lifetime of τ_1 = 7 (±1) ps, (Fig. 5) while the absorbance at position "c" (*vide supra*) reduces simultaneously. The position at lower wavenumbers with respect to the longer-lived transients in the TRIR spectra, lifetime, and broadness suggests that the spectral feature "c" originates from excited states of the $\nu_{as}(N_3)$ vibrations which decay to produce the transient spectrum of the vibrationally relaxed excited state.

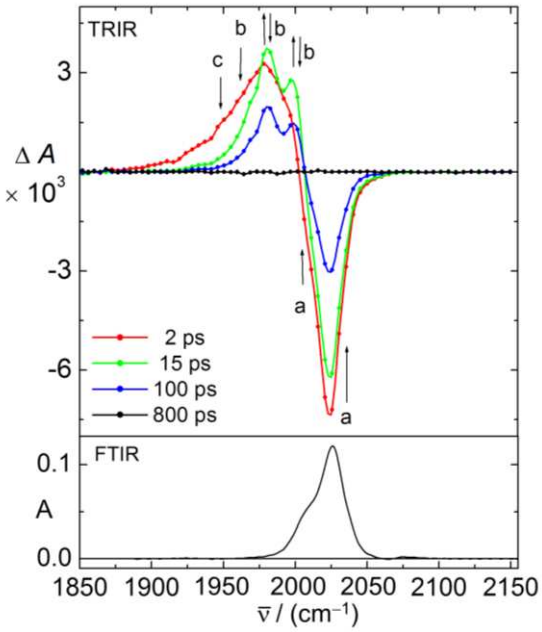

Figure 2. TRIR difference spectra (2 ps – 800 ps) of $Rh(Cp^*)(N_3)_2(PPh_3)$ (**1**) in CH_3CN, λ_{exc} = 400 nm (top); bleached parent bands (a), transient bands (b) and hot bands (c); FTIR spectrum (bottom panel).

The recovery of the bleached parent bands and the decay of all long-lived transients occurs synchronously with a lifetime of τ_2 = 118 (± 15) ps. TRIR spectra of complex **1** in THF (Fig. 3, S3, S12), CH_2Cl_2 and toluene solution (Fig. S11) have similar shapes with minor differences in transient and bleached parent band positions (see Table 1). However, the lifetimes for the decay of vibrationally excited (hot) states vary slightly between τ_1 = 4(±1) ps (CH_2Cl_2) and 6(±1) ps (THF), while the decay of the vibrationally cold transient and the recovery of the bleached parent absorptions have lifetimes as short as 78(±5) ps in toluene.

These findings are interpreted in terms of a set of overlapping bands which arise from vibrationally excited states of an electronic excited state (**1***). The relaxation rate associated with the decay of these bands is solvent-dependent and is progressively slower on moving from MeCN > THF ≈ toluene > CH_2Cl_2. The bands of these excited states are centred at lower energy than those of the vibrational ground state due to anharmonicity. For the $\nu_{as}(N_3)$ stretches the transitions $v = n + 1 \rightarrow v = n + 2$ are therefore at lower wavenumbers than the $v = n \rightarrow v = n + 1$ transitions.

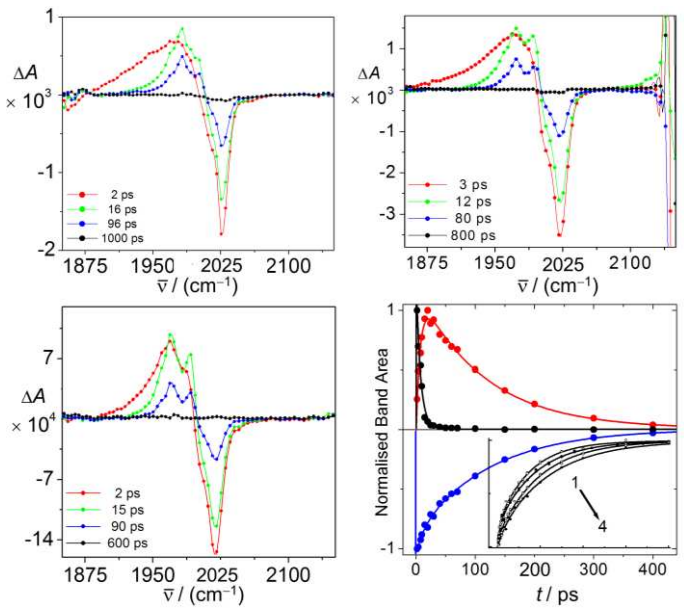

Figure 3. TRIR difference spectra of $Rh(Cp^*)(N_3)_2(PPh_3)$ (**1**): 2 – 1000 ps in MeCN, λ_{exc} = 266 nm (top left), 2 – 800 ps in THF, λ_{exc} = 266 nm (top right); 2 – 600 ps in THF, λ_{exc} = 400 nm (bottom left); normalised kinetic traces of the time-dependent areas of the bands at 1983 cm^{-1} (hot band, black), 2003 cm^{-1}

 This journal is © The Royal Society of Chemistry 2014

(transient, red) and 2026 cm^{-1} (parent, blue) in CH_3CN, λ_{exc} = 400 nm (bottom right; inset: traces of parent bleach recovery in toluene (1), THF (2) CH_2Cl_2 (3), MeCN (4) and in the same time interval).

This assignment is supported by the recently observed anharmonicity in time-resolved 2DIR measurements on azido complexes[38] as well as results from picosecond TRIR for the CO stretching vibrations of short lived intermediates generated by femtosecond excitation of $Rh(Cp)(CO)_2$ where the hot bands have been found *ca*. 40 – 80 cm^{-1} below in energy than the vibrationally cold transient bands.[39,40] Excitation of complex **1** at 400 nm in any of the studied solvents is reversible and the quantum yield for the generation of any reactive intermediate is negligible (Fig. 3). While the excitation of complex **1** in MeCN and THF at higher photon energy (266 nm, see Fig. 3 top left and top right) leads to similar spectral transient features, these are, however, extended much further to lower wavenumbers in the period up to 10 ps after excitation. On the contrary, the TRIR spectra at late time delays, after the cooling process of the electronic excited states is complete, are nearly identical for both excitation energies. This indicates that the excited state detected in TRIR experiments is formed considerably hotter vibrationally if populated with a 266 nm pulse, which in principle could be expected. Importantly, close inspection of the TRIR spectra of **1** (λ_{exc} = 266 nm) reveals residual parent bleach bands which persist at late time indicating irreversible photochemical transformations with estimated quantum yields of 0.033(18) and 0.006(5) in CH_3CN and THF, respectively (Table 1). The nature of the photoproduct could not be ascertained as the long lived transient bands were too weak.

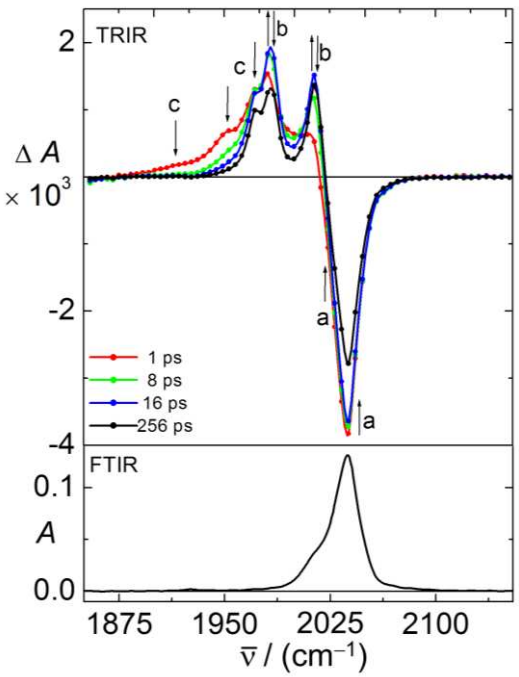

Figure 4. TRIR difference spectra (1 – 256 ps) of $Ir(Cp^*)(N_3)_2(PPh_3)$ (**2**) in MeCN, λ_{exc} = 400 nm; parent bands (a), transient bands (b), and hot bands (c) (top); FTIR spectrum (bottom).

Table 1. Band positions of ground state bleaches and transient absorptions obtained from fits of the TRIR spectra using *pseudo* Voigt profiles (see Fig. 7). Lifetimes of vibrational relaxation (τ_1) and decay (τ_2) of electronic excited state of $M(N_3)_2(Cp^*)(PPh_3)$, M = Rh (**1**), Ir (**2**).

Complex	λ_{exc} / nm	Solvent	$\nu_{as}(N_3)$ parent [a] / cm^{-1}	$\nu_{as}(N_3)$ transient [a] / cm^{-1}	τ_1 / ps	τ_2 / ps	residual parent bleach / % [d]
1	400	CH_3CN	2026, 2007	2003, 1983, 1969	7(±1)	118(±15)	0
1	400	CH_2Cl_2	2025, 2005	2001, 1983, 1968	4(±1)	102(±7)	0
1	400	THF	2022, 2003	1996, 1973, 1960	6(±1)	91(±4)	0
1	400	Toluene	2021, 2002	1995, 1973, 1957	5(±1)	78(±5)	0
1	266	CH_3CN	-	-	5(±1)	129(±11)	3.3(±1.8)
1	266	THF	-	-	4.8(±0.4)	77(±3)	0.6(±0.5)
2	400	CH_3CN	2037, 2017	2015, 1983, 1972	8(±2)	880(±140)	2.1(±0.6)
2	266	CH_3CN	2037, 2017	2015 [b], 1983 [b], 1972 [b]	8(±1)	822(±58)	17(±2)

				2030 [c], 2006 [c]			

[a] position of peak maximum, [b] electronic excited state, [c] permanent photoproduct, [d] (residual bleach) / (total bleach 2 ps after excitation) × 100 %.

The transient spectra of the iridium complex Ir(Cp*)$(N_3)_2(PPh_3)$ (**2**) in MeCN solution (λ_{exc} = 400 nm, Fig.s 4 and S14) are similar to those of the Rh analog discussed above if the time delay 30 ps after excitation is considered. Intriguingly, two comparably broad bands are discernible at low energy, centred at 1919 cm^{-1} and 1954 cm^{-1}, which decay with lifetimes of 4(±1) ps and 8(±1) ps, respectively (Fig. 4, Tab. 1). Spectral position and decay characteristics again match expectations for the vibrationally excited states of the electronic excited state **2*** in which the spectral positions of the absorption bands possibly arise from the transitions $v \rightarrow v+1$ (v = 2, 1919 cm^{-1}; v = 1, 1954 cm^{-1}; v = 0, 1983 cm^{-1}). Fig. 7 shows *pseudo* Voigt fits revealing the precise position and shape of the overlapping bands (see experimental for details).[†] While the vibrational relaxation for the excited states of **2*** resembles that of **1***, the decay of transient bands and parent recovery of τ_2 = 880(±140) ps are approximately seven times slower for the iridium complex (Fig. 5). In contrast, previously reported TRIR studies on the carbonyl complexes M(Cp*)$(CO)_2$ (M = Rh, Ir, λ_{exc} = 295 nm) found no difference for the lifetimes of the excited states.[41,42]

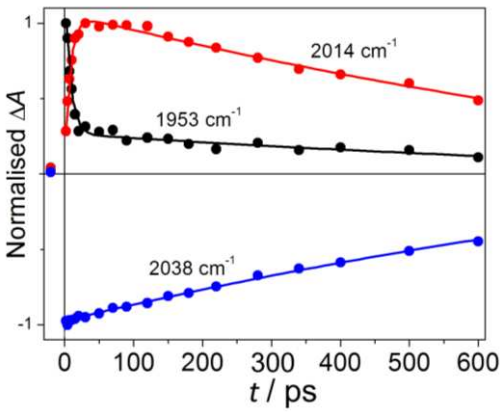

Figure 5. Normalised kinetic traces at 1953 cm^{-1} (black), 1985 and 2014 cm^{-1} (red) and 2038 cm^{-1} (blue) of Ir(Cp*)$(N_3)_2(PPh_3)$ (**2**) in CH_3CN, λ_{exc} = 400 nm; TRIR spectra shown in Fig. 4.

Four nanoseconds after excitation at 400 nm, 98% of the ground state of complex **2** in MeCN solution is recovered (Fig. S7), which suggests the formation of a longer-lived photoproduct with a low quantum yield of less than 0.02. This finding compares well with the quantum yields (0.029-0.067) obtained in steady state photochemical experiments with related complexes Ir(Cp*)$(N_3)_2(PR_3)$, λ_{exc} = 313 nm, in CH_2Cl_2, $CHCl_3$ and C_6H_6 solutions.[9] However, no transient bands of this photoproduct could be discerned in the late time spectra. At a higher excitation energy (λ_{exc} = 266 nm), only 83(2)% of the bleached parent absorption has recovered with two new transient absorption bands being clearly discernible at 2030 cm^{-1} (ν_1) and 2006 cm^{-1} (ν_2), respectively (Fig.s 6, S6). These bands are tentatively assigned to the salt $[Ir(Cp^*)(N_3)(PPh_3)(MeCN)]^+ N_3^-$ (**3**) which is generated upon N_3 / MeCN ligand exchange *via* a coordinatively unsaturated 16e intermediate. This assignment is independently verified by the $\nu_{as}(N_3)$ absorption of the azide anion, which in MeCN appears at 2005 cm^{-1} (ν_2), and by the effect the ligand exchange reaction in the analogous rhodium complex Rh(Cp*)$(N_3)_2(PPh_3)$ *vs*. $[Rh(Cp^*)(N_3)(phen)]^+$ has on the spectral position of the $\nu_{as}(N_3)$ band ν_1 (+4 cm^{-1} to +7 cm^{-1} in nujol).[32] The shift for the average wavenumber of in-phase and out-of-phase $\nu_{as}(N_3)$ vibrations in the proposed complex **3** is +3 cm^{-1}. Alternatively, the 16e intermediate could be saturated by a C(2)-H agostic interaction with phenyl groups of the PPh_3 ligand as observed previously in ruthenium chemistry.[43]

The nearly full reversibility of the photoreaction initiated by excitation at 400 nm and transient lifetimes of less than 1 ns suggest that decay of the electronically excited states ($[M(Cp^*)(N_3)_2(PPh_3)]^{*‡}$, M = Rh, **1***; Ir, **2***) to the ground state is prevailing over possible ligand-loss reactions. The electronic excited state may result from non-dissociative metal-to-ligand charge transfer which would require reduction in the bond order of the N_β-N_γ bonds of the azido ligands thus reducing the force constant of the $\nu_{as}(N_3)$ vibrations in order to agree with the observed transient IR bands which appear at *lower* wavenumber in comparison to the ground state. The occurrence of three transient bands in the excited states **1*** and **2*** apparently contradicts the requirement from first principle according to which diazido complexes cannot have more than two IR active $\nu_{as}(N_3)$ stretches. This issue was investigated by DFT calculations (*vide infra*).

 This journal is © The Royal Society of Chemistry 2014

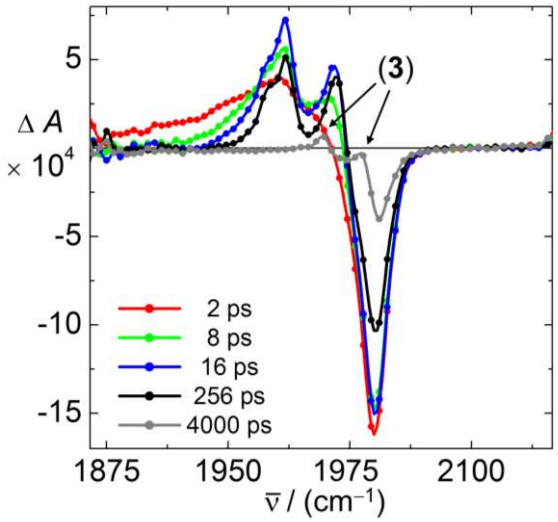

Figure 6. TRIR difference spectra of $Ir(Cp^*)(N_3)_2(PPh_3)$ (**2**) in MeCN solution under 266 nm excitation.

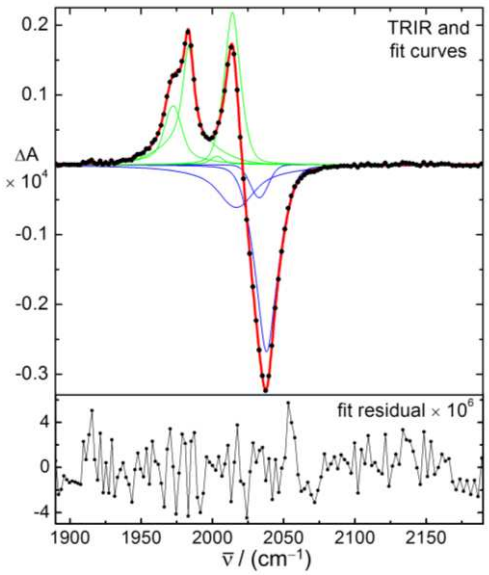

Figure 7. TRIR spectrum obtained *ca*. 512 ps after laser flash (λ_{exc}= 400 nm) (●) of a solution of $Ir(Cp^*)(N_3)_2(PPh_3)$ (**2**) in MeCN. The overlap of *pseudo* Voigt profiles for parent bleach (—) and transient bands (—) results in a fit curve (—) and a residual (—).

Crystallography

A X-ray diffraction study of dark red single crystals of compound **1**, which were obtained from CH_2Cl_2 / hexane at r.t., reveals a complex where rhodium is coordinated by N_3, PPh_3 and Cp* ligands with three-legged piano stool geometry resulting in coordination angles of $Cp^{*(g)}$-Rh-N_α 121.8°, 124.5° and $Cp^{*(g)}$-Rh-P 133.8°, relative to the centre of gravity of the Cp* ring carbon atoms, $Cp^{*(g)}$ (thermal ellipsoid plot shown in Fig. 8). The Cp* ring shows little deviation from planarity (1.9(5) pm) and the coordination centre is located 1.8275(3) Å away from its plane and 1.4 pm off the normal through $Cp^{*(g)}$ indicating a nearly perfect symmetrical η^5 coordination mode. The azido ligands are almost linear (176°, 177°) and coordinate in a fashion typical for terminal non-bridging transition metal azides with Rh-N_α-N_β angles of 119° and 116° and N_α-N_β bonds longer than N_β-N_γ bonds by 5.3(10) pm and 5.8(10) pm, respectively.

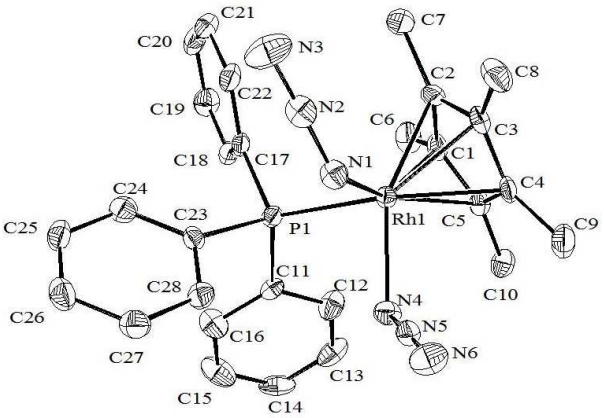

Figure 8. Thermal ellipsoid plot of complex **1** at the 65% probability level; hydrogen atoms are omitted for clarity. Selected bond lengths [Å] and angles [°]: Rh-N1, 2.095(3); N1-N2, 1.210(5); N2-N3, 1.157(5); Rh-N4, 2.132(3); N4-N5, 1.214(4); N5-N6, 1.156(4); Rh-C1, 2.212(4); Rh-C2, 2.173(4); Rh-C3, 2.201(4); Rh-C4, 2.197(4); Rh-C5, 2.197(4); Rh-P, 2.3345(11); N1-Rh-N4, 87.91(16); N1-Rh-P, 88.18(10); N4-Rh-P, 86.93(9).

The latter finding suggests that the Rh-N_α bonds have comparably weak ionic character; however, the low wavenumber for the asymmetric N_3 stretches is close to that of the azide anion and contradicts this notion, unless π back donation is involved which lowers the $\nu_{as}(N_3)$ force constant while maintaining the bond length difference.

DFT Calculations

DFT calculations were employed in order to gain further insight into the nature of the electronic ground and excited states of complexes **1** and **2** and help rationalise the shape of their transient spectra. Using the experimentally determined molecular structure of complex **1** (Fig. 8) as start geometry, three local minima were identified for both rhodium and iridium complex in the singlet ground and first triplet excited states, **1a-c**, **2a-c** and **1a*-c*** and **2a*-c***. These structures are shown in Figs. 9 and S13. While the minimum geometries of **1a** (Fig. 9a) and **2a** (Fig. S13a) closely resemble the structure determined for **1** in the crystal (Fig. 11), other minima are related to these by rotation of azido ligands around the M-N_α bonds (Fig. S13). For each given spin state these rotamers have electronic energies and free energies deviating no more than approximately 8 kJ mol^{-1} from the global minimum and are therefore thermally accessible at r.t. The scaled frequencies calculated for the asymmetric N_3 vibrations (Table 2) were found to reproduce the trends between ground and excited states observed in the TRIR spectra well as can be gleaned from a comparison of Table 1 with Table 2 and Fig. 10.

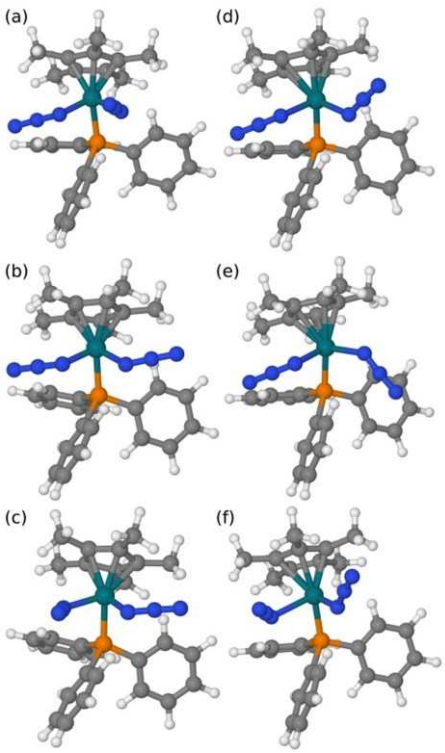

 This journal is © The Royal Society of Chemistry 2014

Figure 9. Rotamers for complex **1** for both the singlet (S_0) ground state and for the first triplet (T_1) state: panel (a) **1a**, panel (b) **1b**, panel (c) **1c**, panel (d) **1a***, panel (e) **1b***, panel (f) **1c***.

Intriguingly, the spread of calculated frequencies of the $\nu_{as}(N_3)$ modes is considerably smaller in the ground state (22, 20 cm^{-1}) than in the excited state (38, 52 cm^{-1}). This result agrees well with the experimentally observed spread, including the fact that **2** has a larger spread in the excited state than **1**. The fact that the ground state IR spectra show only one asymmetric absorption band in the $\nu_{as}(N_3)$ region can therefore be rationalised by the combined effect of the natural linewidth of $\nu_{as}(N_3)$ stretches in solution (FWHM *ca*. 10 cm^{-1}) and the potentially very fast conversion on the vibrational times scale between the rotamers across low activation barriers at r.t.

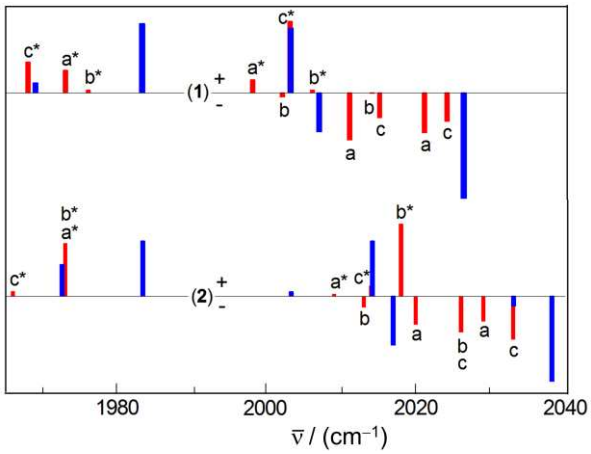

Figure 10. Stick spectra of calculated (red) and observed (blue) vibrational frequencies of $M(Cp^*)(N_3)_2(PPh_3)$ (**1**, M = Rh; **2**, M = Ir) in MeCN. Intensities were adjusted according to the relative abundance of the isomers in the electronic ground (–) and excited states (+) as approximated by their relative Gibbs energies. The electronic ground state intensities are set to negative values.

Table 2. Calculated vibrational frequencies and infrared intensities and relative total and Gibbs energies of the local minima on the singlet ground state and first triplet excited state surface at the B3LYP/6-311g(d,p) level of theory. All frequencies were scaled by 0.955 to account for anharmonicity and correlation effects.

Isomer	$\nu_{as}(N_3)$ / cm^{-1} [a]	ΔE [b]	ΔG [b]
1a	2021 (1977), 2011 (2373)	+1.8	0
1b	2014 (450), 2002 (3774)	+0.6	+7.3
1c	2024 (2346), 2015 (2051)	0.0	+1.2
1a*	1998 (1642), 1973 (2786)	0.0	+2.8
1b*	2006 (2224), 1976 (2162)	+5.6	+7.4
1c*	2003 (2834), 1968 (1219)	+0.8	0
2a	2029 (2015), 2020 (2246)	+1.9	+0.9
2b	2026 (332), 2013 (3912)	0.0	+4.6
2c	2033 (2413), 2026 (2010)	+0.6	0
2a*	2009 (1982), 1973 (2384)	0.0	+5.1
2b*	2018 (2496), 1973 (1820)	+8.0	+8.1
2c*	2014 (2797), 1966 (1297)	+0.9	0

[a] infrared intensities in parentheses, [b] total (E) and Gibbs (G) energies relative to lowest energy rotamer of spin surface in kJ mol^{-1}.

In the excited states, however, individual bands can be resolved since band maxima have larger spectral separation. Therefore, at least two rotamers in the electronic exited states **1*** and **2*** must be assumed to exist in order to rationalise the ps-TRIR observed spectra. Finally, electron density difference plots calculated for the transition of the complexes **1c** and **2c** (see Fig. S16) from the ground to the excited state show on the one hand a reduction in electron density at the metal and on the axis connecting to one N_3 ligand, and on the other hand an increase at the Cp* ligand and between coordination centre and the PPh_3 ligand. Overall, no significant differences could be determined between both complexes. These findings appear to support the suggested metal-to-ligand charge transfer character of the excited state.

Conclusions

The ps-TRIR spectroscopy used to probe light-induced processes in Ir and Rh diazido complexes allows for the direct observation of the vibrationally excited electronic excited states of $M(Cp^*)(N_3)_2(PR_3)$, R = Ph, M = Rh (**1***), Ir (**2***). The excited states **1*** and **2*** are of similar nature, with **2*** possessing a much longer lifetime than **1***, and asymmetric N_3 stretches at lower wavenumbers than the ground state indicating electron donation into antibonding molecular orbitals centred on the azido ligands. DFT calculations in combination with TRIR data suggest that at least two rotamers exist in the excited states of both complexes in

solution. The quantum yields for the generation of long-lived reactive intermediates were found to be close to zero under 400 nm and between 0.06 and 0.17 under 266 nm excitation, depending on the solvent and the central atom. In MeCN solutions of the iridium complex **2** a long lived photoproduct could be identified as a result of heterolytic M-N_3 bond cleavage whereas no analogous photoproduct was formed with the rhodium complex. Overall, the photochemistry of the complexes at the investigated excitation energies is dominated by internal energy conversion (Scheme 1) as opposed to N_2 elimination found in azides, such as DMAP-N_3,[30] with highly covalent azido groups.

Experimental Section

$M(Cp^*)(N_3)_2(PPh_3)$, M = Rh, Ir (**1**, **2**), were synthesized according to published procedures starting from $MCl_3(H_2O)_x$ and 1,2,3,4,5-pentamethylcyclopenta-1,3-diene to afford the dimers $\{M(\eta^5\text{-}Cp^*)Cl_2\}_2$,[31] which is followed by Cl / N_3 exchange and addition of PPh_3 to yield the monomeric diazides **1**[32] and **2**[9]. IR and NMR spectral properties agree with published data. FTIR spectra (4000 - 500 cm^{-1}) were recorded at 2 cm^{-1} resolution; only absorptions larger than one 20th of the $\nu_{as}(N_3)$ band are reported. NMR spectra were recorded at the indicated frequencies and calibrated with the residual ^1H signal (7.26 ppm, 400 MHz) or natural abundance (^{13}C, 77.16 ppm) of the solvent, or externally (^{31}P, 85% H_3PO_4, 101 MHz).

ps-TRIR experiments were performed at the Rutherford Appleton Laboratory (CLF) using the PIRATE and ULTRA laser and detection systems which were described elsewhere.[33, 34] The 266 nm and 400 nm excitations was produced using 3rd and 2nd harmonics of the 50 fs, 800 nm output of the Ti:sapphire amplifier system. The pulse energy at the sample was ~1.5 μJ. The spot sizes of the pump and probe beams were around 150 and 100 μm, respectively. ps-TRIR spectra were obtained by exciting the sample with pump pulses with polarization set at magic angle with respect to the probe. Continuous exchange of the irradiated volume of solution was maintained by recirculating the analyte solution using a peristaltic pump driven, teflon-lined flow system with ~40 ml of solution reservoir in combination with *x*,*y*-rastering to reduce photodegradation at the window solution interface. The ps-TRIR spectra are the difference between the probe spectra when the sample is pumped or not pumped. Probe spectra are acquired at 10 kHz and the sample pumped at 5 kHz. TRIR spectra were calibrated internally using the spectral position of the parent bleach bands. Precise band positions, time-dependent areas and de-convoluted spectral information were obtained using *pseudo* Voigt profiles of the type $y = y_0 + A(\mu(2/\pi)(w_L/(4(x - x_c)^2 + w_L^2)) + \exp(-(4\ln(2)/w_G^2)(x - x_c)^2))$ for each transient and parent bleach absorption band which achieved satisfactory agreement between spectral points and the least squares (χ^2) fit curve (see Fig. 7 as example). Spectral positions and widths of the parent bleach bands were treated as time-independent. Solutions of the complexes with concentrations ranging from 0.8×10^{-3} to 3.7×10^{-3} mol dm^{-3} (**1**) and 0.8×10^{-3} to 6.6×10^{-3} mol dm^{-3} (**2**) were saturated with N_2. Optical densities in the spectroscopic cell at λ = 400 nm and 266 nm, respectively, were kept below unity. An IR Harrick cell spectroscopic cell equipped with CaF_2 windows and optical path lengths ranging from 0.1 to 0.5 mm was used for all TRIR measurements. The solvents THF (spectrometric grade, >99.5 %), CH_3CN (anhydrous, >99.5%), CH_2Cl_2 (spectrophotometric grade, >99.5%), toluene (anhydrous, 99.8%) were used as received from Aldrich or obtained from Grubbs columns[35] (THF, CH_3CN) and were subsequently degassed and stored in ampoules prior to use. The solvent treatment had no influence on the TRIR data. Solutions were degassed, saturated with N_2 and kept under pressure in the recirculating flow system.

Analytical data for compounds **1** and **2**: $Rh(Cp^*)(N_3)_2(PPh_3)$ (**1**): IR $\nu_{as}(N_3)$ [cm^{-1}] = 2005(sh), 2025 (CH_2Cl_2); 2003(sh), 2022 (THF); 2002(sh), 2021 (Toluene); 2007(sh), 2026 (CH_3CN). ^1H NMR ($CDCl_3$, 250 MHz) δ [ppm] = 1.49 ($C_5(CH_3)_5$, 15 H, d, $J_{1H,31P}$ = 3.4 Hz), 7.39-7.53 ($P(C_6H_5)_3$, 15 H, m). $^{13}C\{^1H\}$ NMR ($CDCl_3$, 63 MHz) δ [ppm] = 8.3 ($C_5(CH_3)_5$, s), 128.6 (*meta*-$P(C_6H_5)_3$, d, 10.5 Hz), 131.0 (*para*-$P(C_6H_5)_3$, s), 134.3 (*ortho*-$P(C_6H_5)_3$, d, 10.6 Hz); signals of neither *ipso*-$P(C_6H_5)_3$ nor $C_5(CH_3)_5$ resonances could be discerned. $^{31}P\{^1H\}$ NMR ($CDCl_3$, 101 MHz) δ [ppm] = 34.1 ($P(C_6H_5)_3$, d, $J_{31P,\ 103Rh}$ = 144.4 Hz). $Ir(Cp^*)(N_3)_2(PPh_3)$ (**2**): IR $\nu_{as}(N_3)$ [cm^{-1}] = 2036 (vs, $\nu_{as}(N_3)$), 2013 (w, sh, $\nu_{as}(N_3)$), 1483vw, 1436vw, 1098vw, 1029vw (CH_2Cl_2); 2037, 2017 (sh) (CH_3CN). IR (paraffin, cm^{-1}) ν = 2044 (0.28, sh), 2027 (1.00), 2010 (0.47, sh), 1483 (0.11), 1438 (0.21), 1277 (0.07), 1272 (0.09), 1097 (0.13), 1029 (0.08), 753 (0.12), 705 (0.14), 695 (0.11), 555 (0.05), 530 (0.24). ^1H NMR ($CDCl_3$, 250 MHz) δ [ppm] = 1.54 ($C_5(CH_3)_5$, 15 H, d, $J_{1H,31P}$ = 2.3 Hz), 7.40-7.51 ($P(C_6H_5)_3$, 15 H, m). $^{31}P\{^1H\}$ NMR ($CDCl_3$, 101 MHz) δ [ppm] = 8.2 ($P(C_6H_5)_3$, s).

Crystallographic data for complex **1**: Bruker APEX-II CCD, graphite monochromated Mo($k_{\alpha1,2}$) radiation, λ = 0.71073 Å, $C_{28}H_{30}N_6PRh$, $P2_1/_C$, a = 17.620(4), b = 8.6155(17), c = 17.542(4) Å, $\alpha = \gamma = 90$, β = 98.87(3)°, V = 2631.0(9) Å^3, Z = 4, T = 100(2) K, 0.50 × 0.04 × 0.03 mm, d = 1.475 Mg m^{-3}, F(000) = 1200, μ = 0.739 ($T_{min\ /\ max}$ = 0.7090 / 0.9782), *SADABS* absorption correction, 32677 refl. collected, R(int) = 0.1154, $R(\sigma_I$ /net $I)$ = 0.0931, $-21 \le h \le 22$, $-11 \le k \le 11$, $-22 \le l \le 22$, θ_{min} / θ_{max} = 2.34 / 27.52, 5883 reflections, of which 3946 are > $2\sigma(I)$ with 1 0 0 omitted. The structure was solved by direct methods and refined using the weighting scheme $w = 1 / [s^2 (F_o^2) + (0.0420P)^2 + 0.0000P]$, $P = (F_o^2 + 2 F_c^2) / 3$, 330 parameters, R_1 = 0.0457, wR_2 = 0.1015 (all refl.), GOOF = 0.994, residual diff. density max / min = 0.848 / −1.161.

DFT calculations were performed using Gaussian 09,[36] the B3LYP[44] functional and the 6-311G** basis set[45] for H, C, N, and P. The SDD pseudopotential[46] was used for Rh and Ir. The effects of solvent were included using the polarisable continuum model[47] using the parameters for acetonitrile. In previous work it was found, that this results in a reasonably accurate description of transition-metal complexes and their properties,[48] allowing for semi-quantitative comparison with experiment. The molecular structure found in a crystals of **1** (see Fig. 8) and $Ir(Cp^*)(N_3)_2(PPh_2py)$[37] were used as start geometries for both Ir and Rh complexes for optimisations on the singlet ground state surface.

 This journal is © The Royal Society of Chemistry 2014

These optimised structures served as start geometries for the triplet states. Two more conformers were identified on the triplet surface by adjusting the P-M-N_α-N_β dihedral angles of both azido ligands and were, in turn, used as start structures on the singlet ground state surfaces. For all optimized geometries frequencies were calculated in the harmonic approximation to allow the determination of free energies. No imaginary frequencies were found, confirming that the structures reported on are true minima. A scaling factor of 0.955 was used to compare calculated and experimental frequencies. This factor takes account of anharmonicity and correlation effects not included in our calculation.[49]

Acknowledgements

The authors acknowledge support by EPSRC (fellowship EP / E054978/1 (PP), E-Futures doctoral training centre at the University of Sheffield (BFC)) and STFC through programmatic access "Real-time Structural Dynamics of Molecular Systems for Energy Generation and Storage" (PP, J. A. Weinstein, MT) to the ULTRA facility. I. P. Clark, B. Coles, G. Greetham, I. Sazanovich, J. Best and M. Davis are thanked for their assistance in performing TRIR experiments, R. Campbell and H. Adams for the X-ray analysis, and T. Kane and A. W. Parker for discussions.

Notes and references

[a] Department of Chemistry, University of Sheffield, Brook Hill, Sheffield, S3 7HF, UK. *Email: p.portius@sheffield.ac.uk; Fax: +44 (0)114-22-29346; Tel: +44 (0)114-22-29385.*

[b] Central Laser Facility (CLF), STFC Rutherford Appleton Laboratory, Harwell Science and Innovation Campus, Didcot, Oxfordshire, OX11 0QX, UK.

† The wavenumbers found for the vibrationally excited $\nu_{as}(N_3)$ stretches could be predicted by applying a simplified anharmonic oscillator model: $G(v+1) - G(v) = \omega_e - \omega_e x_e(2v + 2)$, $\omega_e = 2000$ cm^{-1}, $\omega_e x_e = 16$ cm^{-1}.

Electronic Supplementary Information (ESI) available containing additional kinetic data on **1** and **2** in MeCN, CH_2Cl_2, THF and toluene under 266 and 400 nm excitation, TRIR spectra at high and low resolution including *pseudo* Voigt fit profiles, ground state FTIR and UV/*vis* absorption spectra, crystallographic information file as well as coordinates for the different rotamers in XYZ format, see DOI: 10.1039/b000000x/. CCDC 1013155 contains the supplementary crystallographic data for this paper. These data can be obtained free of charge from The Cambridge Crystallographic Data Centre via www.ccdc.cam.ac.uk/data_request/cif.

1. P. C. Samartzis and A. M. Wodtke, *Phys. Chem. Chem. Phys.*, 2007, **9**, 3054.

2. J. Sima, *Coord. Chem. Rev.*, 2006, **250**, 2325-2334.

3. W. P. Fehlhammer and W. Beck, *Z. Anorg. Allg. Chem.*, 2013, **639**, 1053.

4. L. Ronconi and P. J. Sadler, *Chem. Commun.*, 2008, 235.

5. Y.-F. Song, J. F. Berry, E. Bill, E. Bothe, T. Weyhermüller and K. Wieghardt, *Inorg. Chem.*, 2007, **46**, 2208.

6. H. Hennig, R. Stich, H. Knoll, D. Rehorek and D. J. Stufkens, *Coord. Chem. Rev.*, 1991, **111**, 131.

7. A. Vogler, C. Quett and H. Kunkely, *Ber. Bunsen Ges. Phys. Chem.,* 1988, **92**, 1486.

8. J. L. Manson, W. E. Buschmann and J. S. Miller, *Inorg. Chem.*, 2001, **40**, 1926.

9. D. A. Freedman and K. R. Mann, *Inorg. Chem.*, 1991, **30**, 836.

10. G. A. Ozin and J. G. McCaffrey, *J. Am. Chem. Soc.*, 1982, **104**, 7351.

11. A. Vogler and J. Hlavatsch, *Angew. Chem. Int. Ed.*, 1983, **22**, 154.

12. R. S. Paonessa, A. L. Prignano and W. C. Trogler, *Organometallics*, 1985, **4**, 647.

13. D. M. Blake and C. J. Nyman, *J. Am. Chem. Soc.*, 1970, **92**, 5359.

14. A. F. Vaudo, E. R. Kantrowitz, M. Z. Hoffman, E. Papaconstantinou and J. F. Endicott, *J. Am. Chem. Soc.*, 1972, **94**, 6655.

15. D. M. Haddleton, *J. Organomet. Chem.*, 1986, **311**, C21.

16. D. M. Haddleton and R. N. Perutz, *Chem. Commun.*, 1985, 1372.

17. M. W. George, M. B. Hall, O. S. Jina, P. Portius, X.-Z. Sun, M. Towrie, H. Wu, X. Yang and S. D. Zaric, *Proc. Natl. Acad. Sci. U.S.A.*, 2010, **107**, 20178.

18. A. J. Blake, M. W. George, M. B. Hall, J. McMaster, P. Portius, X. Z. Sun, M. Towrie, C. E. Webster, C. Wilson and S. D. Zaric, *Organometallics*, 2008, **27**, 189.

19. M. C. Asplund, P. T. Snee, J. S. Yeston, M. J. Wilkens, C. K. Payne, H. Yang, K. T. Kotz, H. Frei, R. G. Bergman and C. B. Harris, *J. Am. Chem. Soc.*, 2002, **124**, 10605.

20. S. E. Bromberg, H. Yang, M. C. Asplund, T. Lian, B. K. McNamara, K. T. Kotz, J. S. Yeston, M. Wilkens, H. Frei, R. G. Bergman and C. B. Harris, *Science*, 1997, **278**, 260.

21. B. H. Weiller, E. P. Wasserman, R. G. Bergman, C. B. Moore and G. C. Pimentel, *J. Am. Chem. Soc.*, 1989, **111**, 8288.

22. E. P. Wasserman, C. B. Moore and R. G. Bergman, *Science*, 1992, **255**, 315.

23. A. L. Poznyak and V. I. Pavlovski, *Angew. Chem. Int. Ed.*, 1988, **27**, 789.

24. A. Vogler, C. Quett, A. Paukner and H. Kunkely, *J. Am. Chem. Soc.*, 1986, **108**, 8263.

25. H. Hennig, K. Ritter, A. K. Chibisov, H. Görner, F.-W. Grevels, K. Kerpen and K. Schaffner, *Inorg. Chim. Acta*, 1998, **271**, 160.

26. K. McFarlane, B. Lee, J. Bridgewater and P. C. Ford, *J. Organomet. Chem.*, 1998, **554**, 49.

27. M. W. George and P. Portius, *Comprehensive Organometallic Chemistry III, Elsevier: Oxford* 2007, ed. R. H. Crabtree and D. M. P. Mingos, pp. 263-277.

28. P. Portius, A. C. Filippou, G. Schnakenburg, M. Davis and K.-D. Wehrstedt, *Angew. Chem. Int. Ed.*, 2010, **49**, 8013.

29. P. Portius, J. A. Weinstein, M. Davis and I. V. Sazanovich, *CCLRC Central Laser Facility, Rutherford Appleton Laboratory Annual Report, Lasers for Science Facility Programme - Chemistry*, 2009-2010.

30. P. Portius, M. Davis, R. Campbell, F. Hartl, Q. Zeng, A. J. H. M. Meijer and M. Towrie, *J. Phys. Chem. A*, 2013, **117**, 12759.

31. C. White, A. Yates, P. M. Maitlis and D. M. Heinekey, *Inorg. Synth.*, 1992, **29**, 228.

32. W. Rigby, P. M. Bailey, J. A. McCleverty and P. M. Maitlis, *J. Chem. Soc., Dalton Trans.,* 1979, 371.

33. M. Towrie, D. C. Grills, J. Dyer, J. A. Weinstein, P. Matousek, R. Barton, P. D. Bailey, N. Subramaniam, W. M. Kwok, C. Ma, D. Phillips, A. W. Parker and M. W. George, *Appl. Spectrosc.*, 2003, **57**, 367.

34. G. Greetham, P. Burgos, Q. A. Cao, I. P. Clark, P. S. Codd, R. C. Farrow, M. W. George, M. Kogimtzis, P. Matousek, A. W. Parker, M. R. Pollard, D. A. Robinson, Z.-J. Xin and M. Towrie, *Appl. Spectrosc.*, 2010, **64**, 1311.

35. A. B. Pangborn, M. A. Giardello, R. H. Grubbs, R. K. Rosen and F. J. Timmers, *Organometallics*, 1996, **15**, 1518.

36. M. J. Frisch, G. W. Trucks, H. B. Schlegel, G. E. Scuseria, M. A. Robb, J. R. Cheeseman, J. A. Montgomery, J. T. Vreven, K. N. Kudin, J. C. Burant, J. M. Millam, S. S. Iyengar, J. Tomasi, V. Barone, B. Mennucci, M. Cossi, G. Scalmani, N. Rega, G. A. Petersson, H. Nakatsuji, M. Hada, M. Ehara, K. Toyota, R. Fukuda, J. Hasegawa, M. Ishida, T. Nakajima, Y. Honda, O. Kitao, H. Nakai, M. Klene, X. Li, J. E. Knox, H. P. Hratchian, J. B. Cross, V. Bakken, C. Adamo, J. Jaramillo, R. Gomperts, R. E. Stratmann, O. Yazyev, A. J. Austin, R. Cammi, C. Pomelli, J. W. Ochterski, P. Y. Ayala, K. Morokuma, G. A. Voth, P. Salvador, J. J. Dannenberg, V. G. Zakrzewski, S. Dapprich, A. D. Daniels, M. C. Strain, O. Farkas, D. K. Malick, A. D. Rabuck, K. Raghavachari, J. B. Foresman, J. V. Ortiz, Q. Cui, A. G. Baboul, S. Clifford, J. Cioslowski, B. B. Stefanov, G. Liu, A. Liashenko, P. Piskorz, I. Komaromi, R. L. Martin, D. J. Fox, T. Keith, M. A. Al-Laham, C. Y. Peng, A. Nanayakkara, M. Challacombe, P. M. W. Gill, B. Johnson, W. Chen, M. W. Wong, C. Gonzalez and J. A. Pople, *Gaussian Inc. Wallingford, CT*, 2009, Gaussian03.

37. T. Suzuki, M. Kotera, A. Takayama and M. Kojima, *Polyhedron*, 2009, **28**, 2287.

 This journal is © The Royal Society of Chemistry 2014

38. P. Portius and M. Towrie, *unpublished results*, 2012.

39. P. T. Snee, C. K. Payne, K. T. Kotz, H. Yang and C. B. Harris, *J. Am. Chem. Soc.*, 2001, **123**, 2255.

40. J. B. Asbury, H. N. Ghosh, J. S. Yeston, R. G. Bergman and T. Lian, *Organometallics*, 1998, **17**, 3417.

41. S. E. Bromberg, T. Lian, R. G. Bergman and C. B. Harris, *J. Am. Chem. Soc.*, 1996, **118**, 2069.

42. T. P. Dougherty, W. T. Grubbs and E. J. Heilweil, *J. Phys. Chem.*, 1994, **98**, 9396.

43. S. J. L. Placa and J. A. Ibers, *Inorg. Chem.*, 1965, **4**, 778.

44. A. D. Becke, *J. Chem. Phys.*, 1993, **98**, 5648.

45. A. D. McLean and G. S. Chandler, *J. Chem. Phys.*, 1980, **72**, 5639; R. Krishnan, J. S. Binkley, R. Seeger and J. A. Pople, *ibid.* 650.

46. X. Y. Cao and M. Dolg, *J. Chem. Phys.*, 2001, **115**, 7348; A. Nicklass, M. Dolg, H. Stoll and H. Preuss, *ibid*., 1995, **102**, 8942.

47. B. Mennucci and J. Tomassi, *J. Chem. Phys*., 1997, **106**, 5151; M. Cossi, V. Barone, B. Menucci and J. Tomassi, *Chem. Phys. Lett.*, 1998, **286**, 253, and references therein.

48. J. Best, I. V. Sazanovich, H. Adams, R. D. Bennett, E. S. Davies, A. J. H. M. Meijer, M. Towrie, S. A. Tikhomirov, O. V. Bouganov, M. D. Ward and J. A. Weinstein, *Inorg. Chem.*, 2011, **49**, 10041; C. S. Grange, A. J. H. M. Meijer and M. D. Ward *Dalton Trans*., 2010, **39**, 200; S. P. Foxon, C. Green, M. Walker, A. Wragg, H. Adams, J. A. Weinstein, S. C. Parker, A. J. H. M. Meijer and J. A. Thomas, *Inorg. Chem.*, 2012, **51**, 463; J. A. Thomas, H. Ahmad and A. J. H. M. Meijer, *Chem. Asian J.*, 2011, **6**, 2339; A. B. Wragg, S. Derossi, T. L. Easun, M. W. George, X.-Z. Sun, F. Hartl, A. H. Shelton, A. J. H. M. Meijer and M. D. Ward, *Dalton Trans*., 2012, **41**, 10354.

49. K. K. Irikura, R. D. Johnson, R. N. Kacker. *J. Phys. Chem. A*. 2005, **109**, 8430.